Theoretical study of B diffusion with charged defects in strained Si

L. Lin,[1,*] T. Kirichenko,[1,†] B. R. Sahu,[1] G. S. Hwang,[2] and S. K. Banerjee[1]
[1]*Microelectronics Research Center, University of Texas at Austin, Austin, Texas 78758, USA*
[2]*Department of Chemical Engineering, University of Texas at Austin, Austin, Texas 78712, USA*
(Received 4 April 2005; revised manuscript received 25 July 2005; published 15 November 2005)

We investigate B diffusion in strained Si by using density functional theory calculations. We calculate the migration barriers and formation energies of the B-Si complexes at different charge states in the biaxial tensile strained {001} Si layer. The migration barriers and formation energies overall intend to decrease under strain at all charge states. For neutral and negatively charged B-Si complexes, the migration barrier reduces along the strain plane while the barrier in the direction perpendicular to strain plane remains unchanged, but there is no anisotropy in B diffusion for positively charged B-Si complexes.

DOI: 10.1103/PhysRevB.72.205206 PACS number(s): 71.15.−m, 66.30.Jt, 85.40.Ry

I. INTRODUCTION

Strain effect on dopant diffusion has recently received a lot of attention because strained Si/SiGe technology has become very popular due to the enhanced mobility of carriers[1] for next generation metal oxide semiconductor field effect transistors (MOSFETs). Silicon grown on a relaxed SiGe buffer layer is a common embodiment for generating biaxial tensile strain on the Si wafer. Figure 1(a) shows the basic strained Si/relaxed SiGe MOSFET structure.[2] The biaxial tensile strain is induced in the thin epitaxial Si layer by the lattice mismatch between Si and SiGe, and this mismatch depends on the mole fraction of Ge content in SiGe alloy [Figs. 1(b) and 1(c)]. Moreover, with the scaling of MOSFETs, the local process-induced strain can no longer be ignored. The studies of the properties of strained Si such as dopant diffusivity would help develop successful process integration because strain may impact the junction depth of source/drain, and effective channel length of MOSFETs.

Many theoretical and experimental studies have been done about the strain/stress effect on dopant diffusion.[3–13] However, due to the complexity of such experiments, there are many inconsistent, even controversial, experimental results on the effect of strain/stress on diffusion. In the mid-1990's, it was found that B diffusion is suppressed in strained SiGe.[5] Cowern *et al.*[6] proposed that the slower B diffusion is because of the biaxial compressive strain in the SiGe layer grown on the Si substrate. However, Kuo *et al.*[7] found that even for relaxed SiGe, this diffusivity suppression still persists and that B diffusion exhibits weak strain dependence. Recently, Zangenberg *et al.*[8] reported results on strained SiGe and strained Si, which suggested that tensile strain increases the diffusion coefficient of B. One of the reasons for the large variation of experimental data in SiGe is the difficulty of decoupling stress effect and Ge chemical effect. Only the most recent data has clearly attempted to decouple the two factors.[9–13]

Strain can alter many major steps involved in dopant diffusion: formation of native point defects, displacement of a dopant atom to form a mobile dopant complex, and probably clustering of these defects to form extended defects as well.[3] Strain-induced band gap narrowing can also change the charged point-defect concentration.[4] However, there are still a lot of open questions about strain effect on dopant diffusion, such as the effect on the diffusion pathway and migration barrier.

B diffusion in strained Si is an essential topic for understanding strained Si devices. Although many studies of strain/stress effect on B diffusion have been done, the first-principles study of B diffusion in strained Si is still very limited. Our earlier theoretical study[14] confirmed the enhancement and anisotropy of B diffusion in biaxial tensile strained Si for neutral boron-silicon interstitial (B-Si) complex. Although the neutral defects are important, B diffusion is not necessarily a neutral process. We need to study all the charged B-Si complexes to describe B diffusion behavior. Furthermore, we believe that the effect of strain on B diffusion is a combination of elastic stress and band gap narrowing. It is very important to carefully evaluate both of them.

In this paper, only the biaxial tensile strain in strained Si grown on a relaxed SiGe buffer layer is discussed. The strain plane we study is {001} since most of MOSFETs nowadays are fabricated in {001} wafers. Unless otherwise specified, all "strain" refers to biaxial tensile strain on {001} plane.

II. COMPUTATIONAL DETAILS

All the calculations are performed with VASP, which is an *ab initio* quantum-mechanical molecular dynamics simulator based on density functional theory (DFT).[15] The potential used for this calculation is a generalized gradient approximation (GGA) ultrasoft pseudopotential.[16] The simulation is performed on a uniform grid of k points equivalent to a $4\times4\times4$ Monkhorst and Pack grid in the diamond cubic cell. The energy cutoff is 208 eV. Our optimized Si lattice constant for GGA in our system is 5.457 Å. A 64-atom supercell is used. Most of results are also checked in a 216-atom supercell. The differences of migration and formation energies between the two supercells are less than 30 meV.

To introduce biaxial strain in Si, we applied the lattice constant of relaxed $Si_{1-x}Ge_x$ to the two crystallographic directions on the (001) plane ([100] and [010]) since the strained Si grown on relaxed SiGe buffer layer has the same lattice constant as SiGe. We then optimized the lattice constant in the third direction ($a_\perp$) perpendicular to the strain

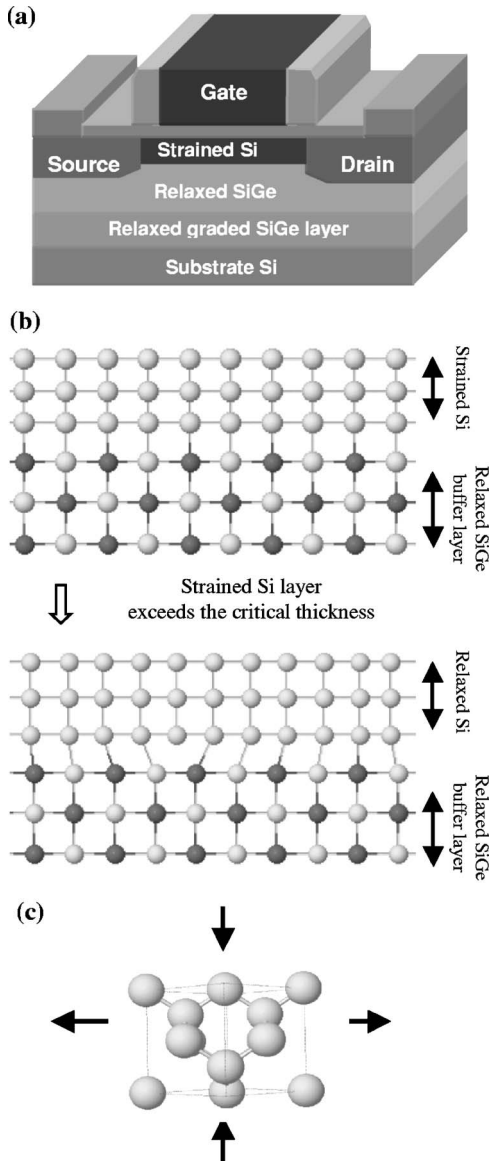

FIG. 1. (a) Schematic diagram of the strained Si MOSFET structure. The Si channel is under biaxial tensile strain. (b) Si can grow epitaxily on SiGe buffer layer with the same lattice constant as SiGe before reaching a critical thickness. This critical thickness is usually a few hundred angstroms. (c) Since the lattice constant of relaxed SiGe is larger than Si, the Si layer grown on SiGe is under biaxial tensile strain.

plane in the 64-atom cell. The lattice constant of relaxed $Si_{1-x}Ge_x$ can be calculated as $a_{SiGe}=(1-x)a_{Si}+xa_{Ge}$, where a_{Si} and a_{Ge} are the lattice constants of Si and Ge, respectively. "In-plane" and "out-of-plane" strain are calculated by $\varepsilon_{\parallel}=(a_{SiGe}-a_{Si})/a_{Si}$ and $\varepsilon_{\perp}=(a_{\perp}-a_{Si})/a_{Si}$. According to the elastic theory,[17] the "in-plane" biaxial strain $\varepsilon_{\parallel}$ can change the "out-of-plane" strain $\varepsilon_{\perp}$ according to the equation

$$\varepsilon_{\perp}/\varepsilon_{\parallel}=-2(C_{12}/C_{11}), \tag{1}$$

where C_{11} and C_{12} are the elastic constants of Si. The experimental values of C_{11} and C_{12} are 167 and 65 GPa, respectively.[18] Our relaxed "out-of-plane" lattice constant and furthermore the calculated $\varepsilon_{\perp}/\varepsilon_{\parallel}$ are in excellent agreement with the experimental values obtained from Eq. (1).

After introducing the defects to the 64-atom supercell, all the atoms in the cell are relaxed to get the minimum energy configuration. The nudged elastic band method (NEBM)[19] determines the minimum barrier energy along its diffusion pathway from the energy difference between the starting point (B-Si complex with the lowest formation energy) and the saddle point. The climbing image method with variable spring constants is used to find the saddle points and minimum energy paths.[20]

The B diffusion coefficient can be written in the Arrhenius form[21,22]

$$D^{BI}=D_0^{BI}\exp(-E_a/\kappa T)=D_0^{BI}\exp[-(H_{BI}^f+H_{BI}^m)/\kappa T] \tag{2}$$

with the prefactor D_0^{BI}, the activation energy E_a, which includes formation enthalpy of stable B-Si complex H_{BI}^f and migration enthaphy H_{BI}^m.

Early DFT studies[23–26] identified B diffusion mechanism in Si based on the energetics of B-Si complexes for various configurations and charge states. The formation energy of defects with charge Q is evaluated as[25,26]

$$E_f^Q=(E_D^Q-E_X^0)+Q(\varepsilon_F+\varepsilon_v)-\sum_s n_s\mu_s, \tag{3}$$

where E_D^Q is the calculated total energy of the supercell containing the defect D, E_X is the total energy of the bulk Si with the same number of atoms as in the defect supercell, ε_F is the Fermi level, and ε_v is the valence band top, which can be calculated by $(E_X^0-E_X^{+1})$. μ_s and n_s are the chemical potential and the number of the atomic species s, respectively.

Since the usual approach to calculate charged defects assumes the introduction of the homogeneous countercharge to keep the neutrality of the supercell, the total energies of charged defects have to be adjusted for the electrostatic interaction between charged defects and the jellium background.[27] For the cubic supercell this correction is equal to[24]

$$E_D^Q(L)=E_D^Q+\frac{\alpha Q^2e^2}{a_0\varepsilon}, \tag{4}$$

where α stands for Madelung constant, and a_0 represents the lattice constant of the supercell. The typical values for this correction are 0.16 and 0.64 eV for singly and doubly charged defects, respectively.

The formation energies of charged defects relative to the neutral state are expressed as[25,26]

$$E_f^{+1}-E_f^0=(E_D^{+1}-E_D^0)+(\varepsilon_v+\varepsilon_F), \tag{5}$$

$$E_f^{-1}-E_f^0=(E_D^{-1}-E_D^0)-(\varepsilon_v+\varepsilon_F). \tag{6a}$$

In Eq. (6a), due to the 50% underestimation of Si band gap in DFT, E_D^{-1} actually includes the information of

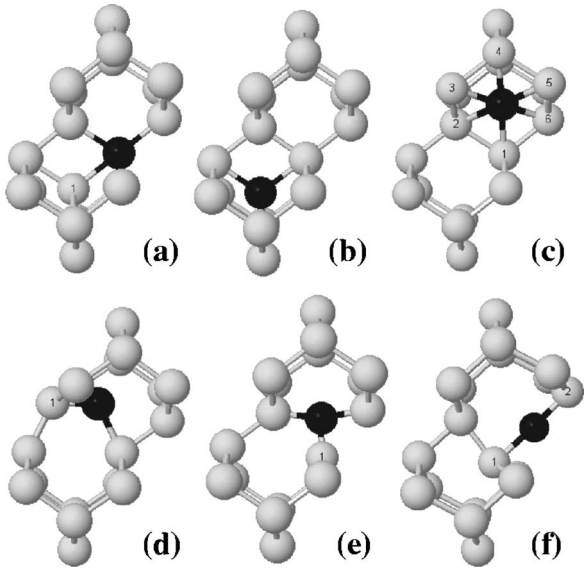

FIG. 2. Atomic B-Si configurations involved in B diffusion. The dark balls represent B atoms. (a) Bs-Si^T, (b) Bi^T, (c) Bi^H, (d) Bi^X, (e) Bi^S, (f) Bi^B.

incorrect band gap. To circumvent this problem to compare our results with experimental observations, we can rewrite Eq. (6a) as

$$E_f^{-1} - E_f^0 = (E_D^{-1} - E_D^0) - (E_X^0 - E_X^{-1}) - \varepsilon_F + E_g, \qquad (6b)$$

where we can use the experimental Si band gap E_g. The above analysis becomes more complicated under strain due to the well-known strain-induced change of Si band gap. The correction of the under-estimation of Si band gap should be carefully applied with the new band gap under strain.

The concentration of charged B-Si complexes can be calculated as[21]

$$C_{\text{B-Si}^+} = C_{\text{B-Si}^0} \exp\left(\frac{E_{\text{B-Si}^+} - E_F}{\kappa T}\right), \qquad (7)$$

$$C_{\text{B-Si}^-} = C_{\text{B-Si}^0} \exp\left(\frac{E_F - E_{\text{B-Si}^-}}{\kappa T}\right), \qquad (8)$$

where C is concentration, B-Si$^{\pm}$ and B-Si^0 are charged and neutral B-Si complexes, and E_F is the Fermi level. The formation energies in Eqs. (5), (6a), and (6b) are directly related to defect energy levels $E_{\text{B-Si}}{}^+$ and $E_{\text{B-Si}}{}^-$.

As a p-type dopant in a semiconductor, B is supposed to provide free "holes." Only in a substitutional site can the B atom be activated to create a free "hole," resulting in a negatively charged B. For B-Si complex, the most stable configuration at neutral state is Bs-Si^T, which is formed by a substitutional B and tetrahedral Si interstitial [Fig. 2(a)]; other configurations, such as B in tetrahedral interstitial site (Bi^T) [Fig. 2(b)] and in hexagonal interstitial site (Bi^H) [Fig. 2(c)], have higher ground state energies. Since Bs-Si^T is the most stable one, we can use high temperature anneal to put B at a substitutional site after implanting B in Si. For the positively charged B-Si complex, Bs-Si^{T+} is still the most stable configuration. At negative charge state, the most stable B-Si complex is Bi^{X-} [Fig. 2(d)]. Bi^X is the configuration that B atom and Si interstitial share one lattice site along the ⟨110⟩ direction. We also mentioned a few other configurations in our calculations, such as Bi^S, in which B and Si share the lattice along ⟨100⟩, and Bi^B in which an interstitial B is located at a bond-centered site, as shown in Figs. 2(e) and 2(f), respectively. They are transition configurations or saddle points along B diffusion pathways.

III. RESULTS AND DISCUSSION

In a strain-free system, B diffusivity can be written as[28]

$$D \approx D^0 + D^+(p/n_i) + D^{2+}(p/n_i)^2 + \cdots + D^-(n/n_i) + D^{2-}(n/n_i)^2 + \cdots, \qquad (9)$$

where $D^0, D^+, D^{2+}, D^-, D^{2-}$ are intrinsic diffusivities associated with neutral, positively and negatively charged defects; p and n are the hole and electron concentrations, respectively; and n_i is the intrinsic carrier concentration. "Intrinsic" Si means Si with no impurities, so p and n are both equal to n_i in intrinsic Si. Experiments show that only the first two terms are major ones in B diffusivity.[28] The positively charged term is as important as the neutral term for the intrinsic condition, and dominates for heavily p-doped conditions. Our calculation results also support this diffusion behavior. As shown in Fig. 3, the negatively charged term is not as important as the neutral and positive ones because the formation energy of the most stable negatively charged B-Si pair is much higher than other charged B-Si complexes. We also provide the formation energies of tetrahedral interstitial Si at different charge states as a function of the Fermi level in Fig. 4.[29,30] In Table I, we summarize all the related energies of the defects at neutral as well as charged states. It suggests that the formation energy of positively charged Bs-Si^T is the lowest. Neutral Bs-Si^T is about 0.2 eV higher, and negative Bi^X is more than 1 eV higher. Here, we choose the Fermi level as 0.6 eV (middle point of the gap) because we are interested in intrinsic condition [as described in Eq. (9)]. The migration energy of neutral Bs-Si^T is 0.45 eV, which is the smallest one among all the B-Si complexes.

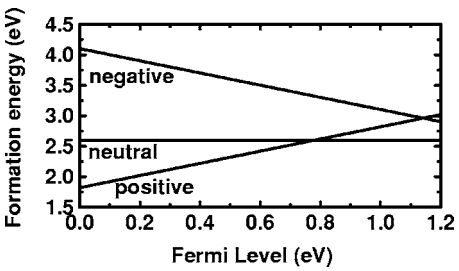

FIG. 3. The formation energies of the most stable B-Si complexes at different charge states with respect to the Fermi level. At neutral and positively charged states, the most stable B-Si complex is B_sI^T, which is formed by a substitutional B and tetrahedral Si interstitial; at negatively charged state, the most stable B-Si complex is B_i^X, which is formed by a B atom and a Si atom sharing one lattice site along [110] direction.

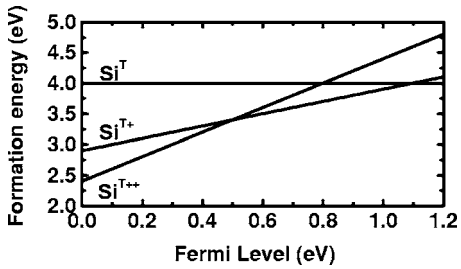

FIG. 4. The formation energies of tetrahedral Si interstitial at different charge states with respect to the Fermi level.

According to Eq. (2), the most favorable diffusion pathway should have the lowest activation energy (that equals to the sum of formation energy and migration barrier). Our results show that under intrinsic condition, although positively charged Bs-Si^T has the lowest formation energy, neutral Bs-Si^T has the lowest activation energy. Figure 5(a) shows the formation energies and migration barriers at different charge states for intrinsic condition. If we assume that B atoms can freely gain/lose electrons during diffusion, the most favorable diffusion pathway[24] should start from Bs-Si^{T+}, which has the lowest formation energy; then Bs-Si^{T+} can acquire an electron and change the charge state to neutral because neutral Bs-Si^T has a much lower diffusion barrier. Therefore, the final activation energy is about 0.65 eV [depending on the Fermi level, ~0.6 eV here]. Figure 5(b) shows the formation energies and migration barriers at different charge states under a highly p-doped condition (where the Fermi level is close to the valence band top, i.e., ~0 eV). From Fig. 5(b), we can clearly see why positively charged defects dominate B diffusion under heavily p-doped conditions. Therefore, for our study of strain effect on B diffusion, it is very important to evaluate all the charged B-Si complexes, not just the neutral ones.

For the neutral B-Si complex, the Bs-Si$^T \rightarrow$ B$i^S \rightarrow$ B$i^H \rightarrow$ B$i^S \rightarrow$ Bs-Si^T path is proposed to be the main migration pathway, as shown in Fig. 6(a). The structures of Bs-Si^T, Bi^S, and Bi^H have been described in Fig. 2. The binding energy of Bs-Si^T is 0.6 eV with respect to the dissociation products B_S^- and Si^{T+}. The diffusion direction from Bs-Si^T to Bi^H is $\langle 113 \rangle$. For the "in-plane" diffusion [[311], [131] with respect to the (001) strain plane], Fig. 6(b) indicates that although the energy of Bi^H changes insignificantly, the saddle point decreases appreciably under a strain of 0.0074, which is related to a $Si_{0.2}Ge_{0.8}$ buffer layer. However, the "out-of-plane" ([113]) migration barrier does not change at all under strain since the entire ground state energies of the B-Si configurations along the pathway shift by almost the same value. The reduction in the "in-plane" diffusion barrier under strain is attributed to the middle configuration Bi^S in which the stretch between B and interstitial Si reduces the repulsive interaction. On the other hand, the compressive strain in the perpendicular direction in the "out-of-plane" case does not lower the migration barrier. Based on the calculations above, there is an anisotropy of diffusion for neutral Bs-Si^T under biaxial tensile strain. Strain can facilitate B diffusion along the strain plane (the channel of MOSFETs).

TABLE I. The migration, formation, and activation energies for differently charged B-Si complexes when Fermi level is at ~0.6 eV from either band edge (middle point of the gap).

	Neutral (Bs-Si^T)	Positive (Bs-Si^{T+})	Negative (Bi^{X-})
$E_{\text{migration}}$ (eV)	0.45	1.0/0.8	0.8
$E_{\text{formation}}$ (eV)	2.6	2.4	3.5
$E_{\text{activation}}$ (eV)	3.05	3.4/3.2	4.1

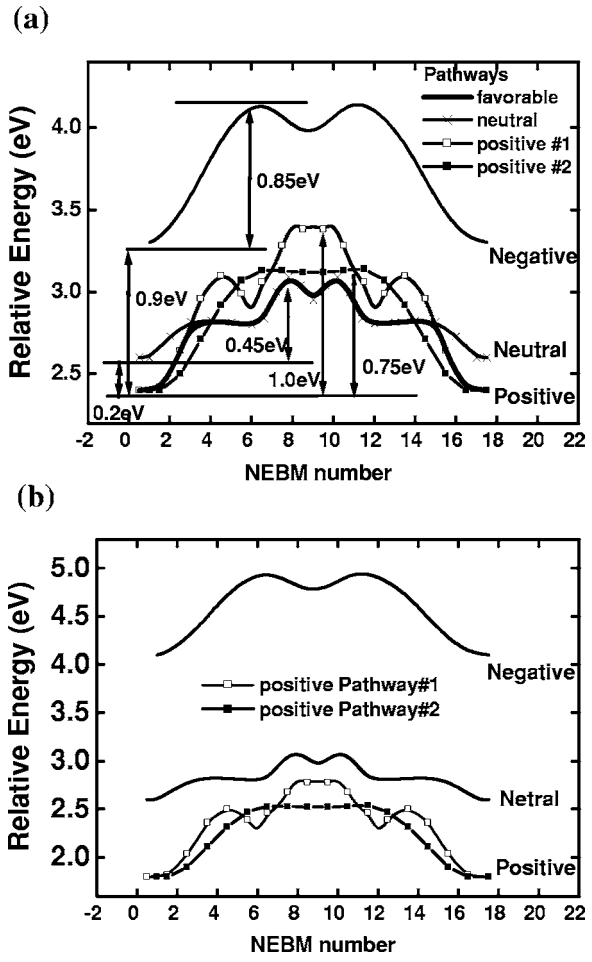

FIG. 5. (a) Formation energies and migration barriers for differently charged B-Si complexes for intrinsic condition (Fermi level is ~0.6 eV). The starting position of each curve depends on the formation energy. The positively charged B-Si complex gains an extra electron in the most "favorable" pathway. (b) Formation energies and migration barriers for differently charged B-Si complexes for heavily p-doped condition (Fermi level is ~0 eV).

The positively charged Bs-Si^T has two competitive pathways (1) Bs-Si$^{T+} \rightarrow$ B$i^{S+} \rightarrow$ B$i^{H+} \rightarrow$ B$i^{S+} \rightarrow$ Bs-Si^{T+} and (2) Bs-Si$^{T+} \rightarrow$ B$i^{B+} \rightarrow$ Bs-Si^{T+}. The first pathway is the same as the neutral pathway. As depicted in Fig. 7(a), the diffusion direction of the second pathway is $\langle 111 \rangle$. The saddle point is Bi^B [Fig. 2(e)]. The binding energy of Bs-Si^{T+} is 0.8 eV, with respect to the dissociation products B_S^- and Si^{T++}. In the second pathway, the Si interstitial [atom No. 1 in Fig. 7(a)] pushes boron from one lattice site to the other along the bond

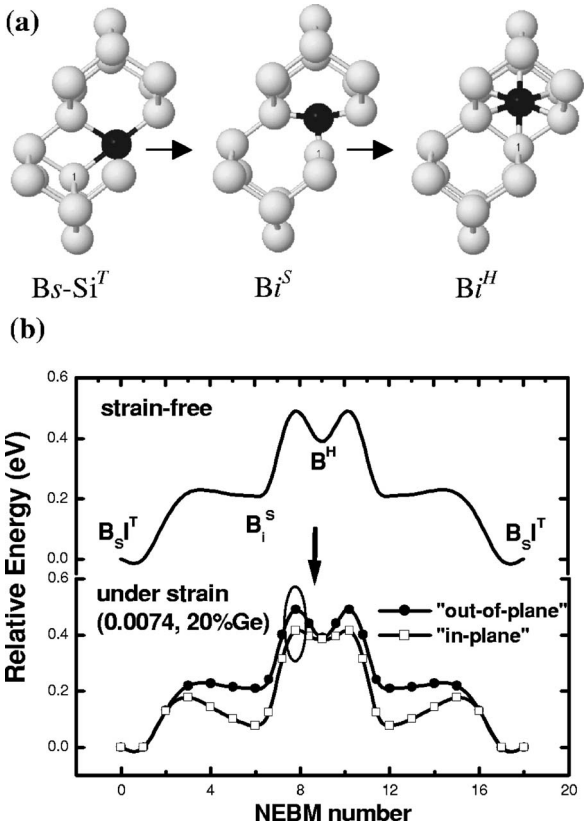

FIG. 6. (a) The first half of the diffusion pathway for neutral Bs-Si^T: Bs-Si$^T \rightarrow$ B$i^S \rightarrow$ Bi^H; then B can diffuse to any of the 6 lattice sites in the hexagonal ring, forming a new Bs-Si^T. (b) The "in-plane" and "out-of-plane" migration barrier under strain for the neutral Bs-Si^T. The strain is 0.0074, which is related to a $Si_{0.8}Ge_{0.2}$ buffer layer.

direction. The Si atom (No. 2) on the other side of B becomes a new Si interstitial. Without any additional steps, following the same diffusion mechanism the new Si interstitial (No. 2) can only reverse boron to the original position (i.e., oscillate back and forth). The second pathway needs to combine with other steps, either other diffusion pathways or additional movements of Si interstitial (No. 2) to help B diffuse to a new site (except the two lattice sites in the dumbbell configuration). Therefore, the real migration barrier of pathway No. 2 for multiple-step diffusion depends on the additional movement of Si interstitial, which has a barrier about 1.1 eV (from one tetrahedral interstitial position to a nearby tetrahedral interstitial position), higher than the migration energy of the second pathway (0.8 eV). This is also mentioned in Ref. 25.

For the first pathway, the "out-of-plane" migration barrier remains unchanged. Unlike the neutral case, the "in-plane" barrier does not change also because the saddle point Bi^{H+} stays at the same value, although the relative energies of some middle points decrease, as shown in Fig. 7(b). Bs-Si^T has C_{3v} symmetry. The $\langle 111 \rangle$-symmetry axis makes all the Bs-Si^T configurations equivalent with respect to the biaxial strain plane. Bi^H has a D_{3d} symmetry, which also has a $\langle 111 \rangle$-symmetry axis. Both of them are intrinsically isotropic. The difference between the neutral and positively

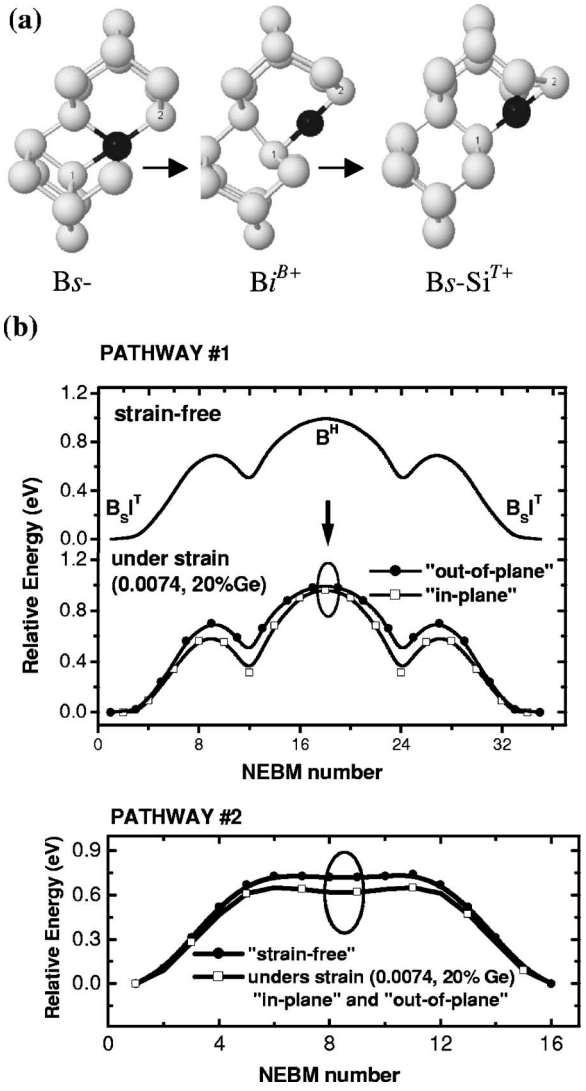

FIG. 7. (a) The second diffusion pathway for positively charged Bs-Si^T: Bs-Si$^{T+} \rightarrow$ B$i^{B+} \rightarrow$ Bs-Si^{T+} (the first pathway is as same as neutral pathway). (b) The change of migration barriers under strain for positively charged Bs-Si^T. The strain is 0.0074, which is related to a $Si_{0.8}Ge_{0.2}$ buffer layer.

charged Bs-Si^T for the same diffusion pathway arises from the fact that Bi^H is not the saddle point in the neutral case. The real saddle point in the neutral case is not isotropic and affected by the middle configuration Bi^S which has a C_2 symmetry. There is a reduction in the migration barrier for the second pathway [Fig. 7(b)] because tensile strain relaxes the local stress of the saddle point Bi^B. Since the symmetry axis of Bi^B is $\langle 111 \rangle$, the decrease of migration barrier is isotropic for biaxial tensile strained Si with a (100) strain plane. Therefore, both diffusion pathways of positively charged Bs-Si^T do not show an anisotropy of B diffusion and only the second pathway has a lower migration barrier under strain.

For the negatively charged case, Bs-Si^{T-} is unstable. The most stable B-Si complex is Bi^{X-}, as shown in Fig. 2(f). The pathway B$i^{X-} \rightarrow$ B$i^{S-} \rightarrow$ Bi^{X-} [Fig. 8(a)] is the most favorable one. The diffusion direction is $\langle 110 \rangle$. Because of the transi-

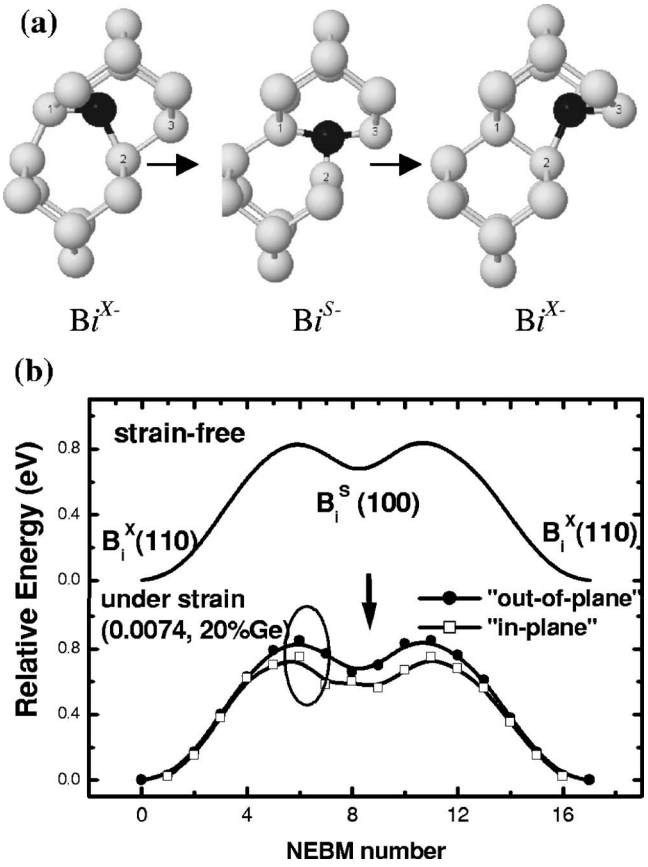

FIG. 8. (a) The diffusion pathway $Bi^{X-} \rightarrow Bi^{S-} \rightarrow Bi^{X-}$ for negatively charged Bi^X. (b) The "in-plane" and "out-of-plane" migration barriers under strain for negatively charged Bi^X. The strain is 0.0074, which is related to a $Si_{0.8}Ge_{0.2}$ buffer layer.

tion point Bi^{S-}, we found a similar effect of strain as on the neutral diffusion pathway. The "in-plane" [[110] with respect to the (001) strain plane] barrier is reduced, while the "out-of-plane" ([011] and [101]) barriers remain unchanged [Fig. 8(b)].

For some major defects in B diffusion, Fig. 9 shows the effect of strain on the ground-state energies at different charge states. The energy of Si^{T++} increases with strain, while Si^{T+} has a similar dependence on strain as pure Si does and the energy of neutral Si^T decreases. (The change of pure

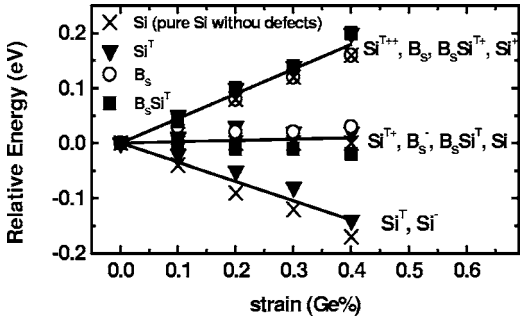

FIG. 9. The ground-state energy dependence on strain for differently charged defects in 64-atom supercell. Neutral pure Si is used as the reference.

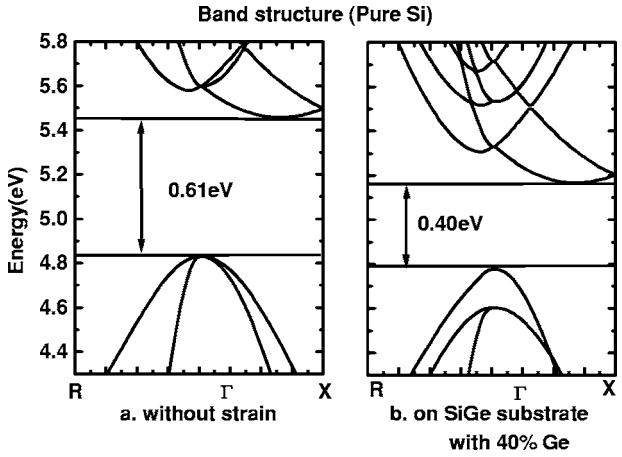

FIG. 10. The band structure of pure Si in 64-atom supercell without and with strain.

Si with strain is used as the reference here.) This behavior is due to a combination of elastic stress and band gap narrowing. For the migration barriers, the energy dependence on the charge states is not important because we are just interested in the same charge state. However, for the effect of strain on the formation energies, we have to carefully evaluate the energy changes under strain associated to different charge states.

In order to explain the ground state energy dependence on strain of pure Si and other defects, we have studied the changes of band structure and density of states (DOS) with strain.[31] Since the strain range in this study is with respect to a SiGe buffer layer in which mole fraction of Ge changes from 0–40 %, we use the largest strain (40% Ge) here. Figure 10 shows that the band gap indeed decreases, in agreement with other calculations.[32] The band gap narrowing mainly results from the lowering of the conduction band; the valence band edge remains nearly unchanged. This results in that the energy of negatively charged Si, which has one extra electron in conduction band, should decrease with strain (Fig. 9).

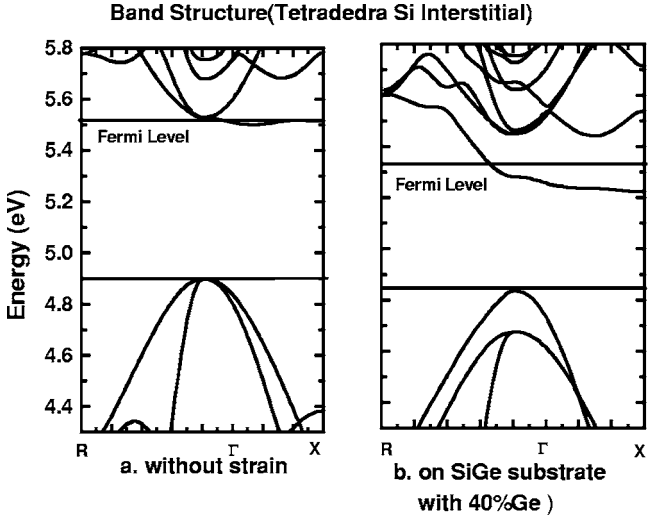

FIG. 11. The band structure of tetrahedral Si interstitial in 64-atom supercell without and with strain.

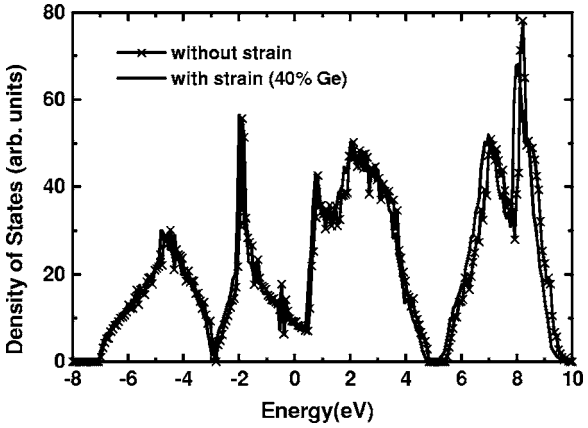

FIG. 12. Density of states (DOS) of pure Si in 64-atom supercell without and with strain.

A tetrahedral Si interstitial has two *s*-electrons that should be in the valence band, and the two *p* electrons should be in the defect energy level near conduction band, as shown in Fig. 11. Below the Fermi level, there is one defect energy level. Because of spin degeneracy, it can occupy two electrons. For neutral Si^T, it is obvious from Fig. 11 that the energies of these two electrons decrease with strain. It explains why the energy of neutral Si^T decreases under strain with respect to neutral pure Si (Fig. 9).

Although the peak of valence band almost stays at the same position with strain (Fig. 10), the energy of positively charged Si, which has one hole at the edge of valence band, still increases with strain with respect to neutral Si (Fig. 9). To understand this, we have done the DOS calculation of pure Si (Fig. 12). The DOS shifts slightly to a lower value under strain, suggesting the valence band edge at other *k* points decrease more than at the Γ point. Since our calculations have been done in a $4\times4\times4$ *k*-point mesh, not just Γ or *X* point, it is possible that the energy of the positively charged Si supercell increases with strain when there is a hole at the edge of the valence band.

Based on the above analysis and Eqs. (3)–(5), (6a), and (6b), we find that all the formation energies of the most stable B-Si complexes are reduced by strain under the intrinsic condition (Table II). The formation energies of charged B-Si complexes decrease more than the neutral one. Finally, we can get all the changes of formation energies as well as migration barriers of B-Si complexes at different charge states, as shown in Table II. Basically the trend of decreasing "in-plane" migration barriers and the resulting anisotropy of B diffusivities persist for neutral and negatively charged B-Si complexes. For positively charged B-Si complex, although the migration barrier reduces in the second pathway, there is no anisotropy in B diffusion.

TABLE II. The changes of migration and formation energies for differently charged B-Si complexes under strain in intrinsic condition with respect to the unstrained system. The strain is 0.0074, which is related to Si grown on a $Si_{0.8}Ge_{0.2}$ buffer layer, and the diffusivity is for 1000 °C. (The positively charged B-Si complex has two competitive diffusion pathways.)

		Neutral	Positive	Negative
$\Delta E_{\text{migration}}$ (eV)	In-plane	−0.1	0/−0.1	−0.1
	Out-of plane	0	0/−0.1	0
$\Delta E_{\text{formation}}$ (eV)		−0.1	−0.15	−0.15
Diffusivity enhancement	In-plane	~4	~3/5	~5
	Out-of plane	~2	~3/5	~3

Moreover, strain can also reduce the difference in the formation energies of differently charged defects under heavily *p*-doped condition due to band gap narrowing, which can be seen easily from Eqs. (7) and (8). This leads to a relatively weak doping concentration dependence of B diffusion under strain. Since $n_i=\sqrt{N_cN_v}e^{-E_g/2kT}$, we can also write the first two terms of Eq. (9) as $D^0+D^+(p/n_i)e^{\Delta E_g/kT}$.[4] Here N_c and N_v are the density of states at the conduction and valence band edge, respectively; n_i is the intrinsic electron concentration in unstrained Si; and ΔE_g is the change of band gap due to the strain. Since ΔE_g is negative, we can also conclude a weak doping concentration dependence of B diffusion in strained Si under heavily *p*-doped conditions.

IV. CONCLUSIONS

We have studied the effect of strain on B diffusion for differently charged B-Si complexes. In biaxial tensile strained Si, B diffusion is enhanced at all three charge states (neutral, positive, and negative). Furthermore, there exists an anisotropy in B diffusion under biaxial strain for neutral and negatively charged B-Si complexes. But for positively charged B-Si complex, no anisotropy of migration barrier is found. This leads to less anisotropic diffusion in strained Si in heavily *p*-doped conditions. The difference in defect formation energies under heavily *p*-doped conditions also decreases because of band gap narrowing. The strain effect on B diffusion is attributed to a combination of elastic stress and band gap narrowing.

ACKNOWLEDGMENTS

This work was supported in part by Texas Advanced Materials Research Center, Texas Instruments, Micron Technology, and the Texas Advanced Technology Program.

*Email address: llin@ece.utexas.edu
†Present address: Freescale Semiconductor, 3501 Ed Bluestein Blvd., Austin, TX 78712, USA.

[1] F. Schaffler, Semicond. Sci. Technol. **12**, 1515 (1997).
[2] G. Xia, H. M. Nayfeh, M. L. Lee, E. A. Fitzgerald, D. A. Antoniadis, D. H. Anjum, J. Li, R. Hull, N. Klymko, and J. L. Hoyt, IEEE Trans. Electron Devices **51**, 2136 (2004).
[3] S. Chaudhry and M. Law, J. Appl. Phys. **82**, 1138 (1997).
[4] N. Moriya, L. C. Feldman, H. S. Luftman, C. A. King, J. Bevk, and B. Freer, Phys. Rev. Lett. **71**, 883 (1993).
[5] P. Kuo, J. L. Hoyt, J. F. Gibbons, J. E. Turner, R. D. Jacowitz, and T. I. Kamins, Appl. Phys. Lett. **62**, 612 (1993).
[6] N. E. B. Cowern, P. C. Zalm, P. van der Sluis, D. J. Gravesteijn, and W. B. de Boer, Phys. Rev. Lett. **72**, 2585 (1994).
[7] P. Kuo, J. L. Hoyt, J. F. Gibbons, J. E. Turner, and D. Lefforge, Appl. Phys. Lett. **66**, 580 (1995).
[8] N. R. Zangenberg, J. Fage-Pedersen, J. L. Hansen, and A. N. Larsen, J. Appl. Phys. **94**, 3883 (2003).
[9] Y. Zhao, M. J. Aziz, Hans-J. Gossmann, S. Mitha, and D. Schiferl, Appl. Phys. Lett. **74**, 31 (1999).
[10] M. S. Daw, W. Windl, N. N. Carlson, M. Laudon, and M. P. Masquelier, Phys. Rev. B **64**, 045205 (2001).
[11] M. Laudon, N. Nd. Carlson, M. P. Masquelier, M. S. Daw, and W. Windl, Appl. Phys. Lett. **78**, 201 (2001).
[12] W. Windl, M. Laudon, N. N. Carlson, and M. S. Daw, Comput. Sci. Eng. **3**, 92 (2001).
[13] M. Diebel and S. T. Dunham, *IEEE International Conference on Simulation of Semiconductor Processes and Devices (SISPAD)*, Boston, Massachusetts, 2003 (IEEE, 2003), pp. 147–150.
[14] L. Lin, T. Kirichenko, G. Hwang, and S. Banerjee, J. Appl. Phys. **96**, 5543 (2004).
[15] G. Kresse and J. Hafner, Phys. Rev. B **47**, R558 (1993); **49**, 14251 (1994); G. Kresse and J. Furthmuller, Comput. Mater. Sci. **6**, 15 (1996); Phys. Rev. B **54**, 11169 (1996).
[16] J. P. Perdew, K. Burke, and M. Ernzerhof, Phys. Rev. Lett. **77**, 3865 (1996).
[17] C. G. Van de Walle and R. M. Martin, Phys. Rev. B **34**, 5621 (1986).
[18] M. E. Levinshtein, S. L. Rumyantsev, and M. S. Shur, *Handbook Series on Semiconductor Parameters* (World Scientific, London, 1996), Vol. 1, p. 29.
[19] H. Jonsson, G. Mills, and K. W. Jacobsen, in *Classical and Quantum Dynamics in Condensed Phase Simulations*, edited by B. J. Berne, G. Ciccotti, and D. F. Coker (World Scientific, Singapore, 1998), p. 385.
[20] G. Henkelman, B. P. Uberuaga, and H. Jónsson, J. Chem. Phys. **113**, 9901 (2000).
[21] P. M. Fahey, P. B. Griffin, and J. D. Plummer, Rev. Mod. Phys. **61**, 289 (1989).
[22] J. Zhu, T. D. dela Rubia, L. H. Yang, C. Maihiot, and G. H. Gilmer, Phys. Rev. B **54**, 4741 (1996); J. Zhu, Comput. Mater. Sci. **12**, 309 (1998).
[23] B. Sadigh, T. J. Lenosky, S. K. Theiss, M-J. Caturla, T. Diaz de la Rubia, and M. A. Foad, Phys. Rev. Lett. **83**, 4341 (1999).
[24] W. Windl, M. M. Bunea, R. Stumpf, S. T. Dunham, and M. P. Masquelier, Phys. Rev. Lett. **83**, 4345 (1999).
[25] J. W. Jeong and A. Oshiyama, Phys. Rev. B **64**, 235204 (2001).
[26] M. Hakala, M. J. Puska, and R. M. Nieminen, Phys. Rev. B **61**, 8155 (2000).
[27] P. A. Schultz, Phys. Rev. Lett. **84**, 1942 (2000).
[28] S. K. Ghandhi, *VLSI Fabrication Principles: Silicon and Gallium Arsenide* (Wiley, New York, 1994).
[29] G. M. Lopez and V. Fiorentini, Phys. Rev. B **69**, 155206 (2004).
[30] W.-K. Leung, R. J. Needs, G. Rajagopal, S. Itoh, and S. Ihara, Phys. Rev. Lett. **83**, 2351 (1999).
[31] W. Windl, Phys. Status Solidi B **241**, 2313 (2004).
[32] M. V. Fischetti and S. E. Laux, J. Appl. Phys. **80**, 2234 (1996).